Engineering Applications of Artificial Intelligence 68 (2018) 153–164

Contents lists available at ScienceDirect

Engineering Applications of Artificial Intelligence

journal homepage: www.elsevier.com/locate/engappai

Classification of Upper limb phantom movements in transhumeral amputees using electromyographic and kinematic features

Guillaume Gaudet [a,b,*], Maxime Raison [a,b], Sofiane Achiche [a]

[a] *Department of mechanical engineering, École Polytechnique de Montréal, 2900 Boul. Édouard-Montpetit, Montreal (Qc), Canada H3T 1J4*

[b] *Rehabilitation Engineering Chair Applied in Pediatrics (RECAP), Marie Enfant Rehabilitation Centre, 5200 Bélanger, Montreal, Quebec, Canada H1T1C9*

A R T I C L E I N F O

Keywords:
Surface electromyography (sEMG)
Pattern recognition
Phantom limb movements
Transhumeral amputee
Neural networks
Classification

A B S T R A C T

Recent studies have shown the ability of transhumeral amputees to generate surface electromyography (sEMG) patterns associated to distinct phantom limb movements of the hand, wrist and elbow. This ability could improve the control of myoelectric prostheses with multiple degrees of freedom (DoF). However, the main issue of these studies is that these ones record sEMG from sites that cannot always be integrated in a prosthesis socket. This study aims to evaluate the classification accuracy of eight main upper limb phantom movements and a no movement class in transhumeral amputees based on sEMG data recorded exclusively on the residual limb. A sub-objective of this study is to evaluate the impact of kinematic data on the classification accuracy. Five transhumeral amputees participated in this study. Classification accuracy obtained with an artificial neural network ranged between 60.9% and 93.0%. Accuracy decreased if the number of DoF considered in the classification increased, and/or if the phantom movements became more distal. Adding a kinematic feature produced an average increase of 4.8% in accuracy. This study may lead to the development of a new myoelectric control method for multi-DoF prostheses based on phantom movements of the amputee and kinematic data of the prosthesis.

1. Introduction

Upper limb amputation causes substantial functional impairments for patients, which increases as the level of amputation is located higher up the arm (Gaine et al., 1997). Indeed, most activities of daily living, such as tying shoelaces, opening a bottle, and buttoning a shirt, are complex and are hard to accomplish with only one fully functional arm. However, some amputees still choose to wear only a cosmetic prosthesis, without any functional utility, even though active prostheses are nowadays capable of restoring some functions, but these ones are sometimes too unnatural to use (Pulliam et al., 2011).

The two predominant types of active prostheses for transhumeral amputees are body-powered and myoelectric (Carey et al., 2015). In body-powered prostheses, a functional body harness allows the amputee to actuate the prosthesis by performing specific shoulder motions. In contrast, myoelectric prostheses are controlled by the surface electromyography (sEMG) signals produced by the residual muscles of the amputee. In some cases, there can be a combination of both options: a body-powered elbow with a myoelectric wrist and hand. While body-powered prostheses provide limited functionality, myoelectric prostheses have the potential to offer intuitive control and could act on multiple degrees of freedom (DoF).

Current clinical strategies for myoelectric control are based on direct control, which does not allow intuitive and simultaneous control of multiple DoF prostheses (Young et al., 2013). Direct control is based on the amplitude of two antagonist muscles, such as the biceps brachii and the triceps brachii, and acts on a single DoF. For transhumeral amputees, at least three DoF prostheses are necessary to maintain minimal functionality: elbow flexion–extension, forearm pronation–supination and hand open–close. Moreover, a fourth DoF, wrist flexion–extension, should also be integrated in myoelectric prostheses, considering it is an area of dissatisfaction for users (Biddiss et al., 2007). Simultaneous control of these four DoF is almost impossible using a direct control strategy since transhumeral amputees do not possess enough independently controllable muscles left in their residual limb (Parker et al., 2004). To overcome this problem, the preferred strategy is to employ co-contraction of the muscles or hardware switches to move from one DoF to another (Scheme and Englehart, 2011). Hence, the dexterity of control is limited, slow, and counterintuitive, which explains the low acceptance of myoelectric prosthesis (Biddiss et al., 2007; Carey et al., 2015).

* Corresponding author at: Department of mechanical engineering A-530, École Polytechnique de Montréal, 2900 Boul. Édouard-Montpetit, Montreal (Qc), Canada H3T 1J4.
E-mail address: guillaume.gaudet@polymtl.ca (G. Gaudet).

https://doi.org/10.1016/j.engappai.2017.10.017
Received 18 April 2017; Received in revised form 31 August 2017; Accepted 21 October 2017
0952-1976/

The actual limitations of the direct control strategy have motivated the use of a pattern recognition-based control (Hudgins et al., 1993). Pattern recognition requires that more information must be extracted from the residual muscles. To do so, it is recommended to use multiple channels of surface electromyography (sEMG) and to use a feature set that extract as much information as possible from the sEMG signals (Englehart and Hudgins, 2003). Feature extraction aims to extract the valuable information that is hidden in sEMG signal (Phinyomark et al., 2013). The extracted features are then processed by a classifier, which role is to decide to which class the information belongs. For myoelectric control, each class corresponds to a single movement of the prosthesis.

Several studies successfully used a pattern recognition approach to classify upper limb movements (Englehart and Hudgins, 2003; Hargrove et al., 2007; Herle et al., 2012; Pulliam et al., 2011; Young et al., 2013). However, few of them were realized on actual transhumeral amputees (Young et al., 2013; Hudgins et al., 1993; Tkach et al., 2012). This is a major shortcoming as it is known that EMG activity in the residual limb differs from the one in the intact limb (Reilly et al., 2006). Moreover, there is more interest for amputees who underwent targeted muscle reinnervation (TMR) surgery (Kuiken et al., 2007) because this procedure allows to transfer residual arm nerves to alternative muscles sites, increasing the number of sites for sEMG recordings. However, the potential risks associated with TMR are considerable: permanent paralysis of the target muscles, development of painful neuromas and recurrence of phantom limb pain (Kuiken et al., 2007). Therefore, it is crucial to assess the accuracy of a pattern recognition approach on actual transhumeral amputees who did not undergo TMR surgery.

Recent studies have shown that transhumeral amputees can produce different muscle activation patterns that are related to distinct phantom movements and that physiologically inappropriate muscles can produce phantom movements required to myoelectric control (Gade et al., 2015; Jarrasse et al., 2016). Indeed, it is known that multiple neuromuscular reorganizations occur after the amputation (Cohen et al., 1991) and that the primary motor cortex can still send motor commands to the missing limb (Mercier et al., 2006). Moreover, there is a high proportion of upper limb amputees that experience phantom limb sensations (De Graaf et al., 2016). This ability could improve the control of multiple DoF myoelectric prostheses without undergoing muscular re-innervation surgery. However, the main issue of these studies is that these ones record sEMG from sites that cannot always be integrated in a prosthesis socket, such as shoulder, back, and pectoralis muscles.

Latest developments on myoelectric prostheses propose to combine myoelectric signal with other sensory or biological signals to improve the control of prostheses (Madusanka et al., 2015). These additional inputs can come from electroencephalography (Bell et al., 2008), electrocorticography (Kubánek et al., 2009), foot pressure sensors (Resnik et al., 2014), vision (Madusanka et al., 2015), and inertial measurement units (Fougner et al., 2011a). Among these, inertial measurement units, such as accelerometers, require the simplest hardware and can easily be integrated at different locations on a prosthesis, giving precious information about its orientation, speed and acceleration. This kinematic information, combined with sEMG features, could improve the accuracy of current pattern recognition classifiers (Fougner et al., 2011b; Radmand et al., 2014).

In this study, we evaluate the accuracy of a state-of-the-art classifier to classify eight upper limb phantom movements and a no movement class in transhumeral amputees using sEMG and kinematic features. sEMG data were recorded exclusively from sites that can be integrated in a prosthesis socket to facilitate the transfer in actual prostheses. Therefore, no sEMG was recorded from the deltoid, trapezoidal, back or pectoralis muscles, as it was the case in most recent studies investigating upper limb phantom movements (Gade et al., 2015; Jarrasse et al., 2016). The impact of kinematic data on classification accuracy was also evaluated.

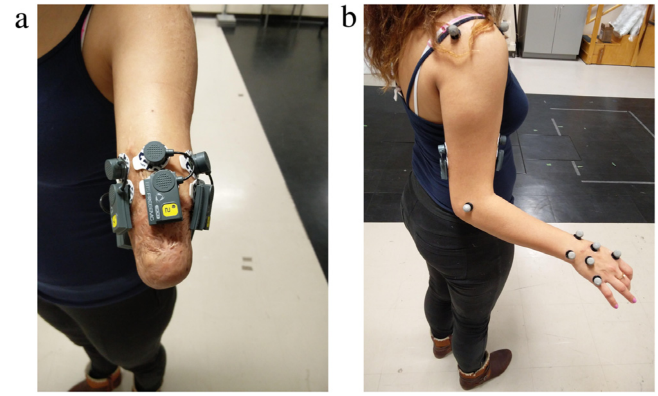

Fig. 1. Placement of (a) 6 sEMG channels and (b) 10 retroreflective markers on one transhumeral amputee.

2. Methods

2.1. Participants

Five participants with unilateral traumatic transhumeral amputation volunteered to participate in the study (Table 1). Participants provided informed consent and permissions to publish photographs. The study was approved by the Research Ethics Board of Ste-Justine University Hospital Center, Montreal, Canada.

2.2. Data acquisition

Six sEMG channels equally spaced around the stump (Fig. 1a) were recorded for each participant using the wireless FreeEMG300 system (BTS, Milan, Italy) and BTS EMG-Analyzer (BTS, Milan, Italy) software, with the following specifications: sampling frequency: 1 kHz; gain: 476.5; CMRR>110 dB; input impedance >10 GOhm; high-pass pre-filtered 7.32 Hz −20 dB·s^{-1}; 16-bit resolution. The skin overlying the electrode sites was scrubbed using 70% isopropyl alcohol pads to reduce electrode resistance and disposable self-adhesive bipolar circular electrodes (Ag/AgCl, recording diameter, 10 mm; center-to-center distance, 24 mm; Covidien, Mansfield, USA) were used for sEMG recordings.

Kinematics data were recorded by a 12-camera 3D motion analysis system (T40Sx VICON, Oxford) at a sampling frequency of 100 Hz. Ten retro-reflective markers were placed on the following anatomical landmarks of the intact limb (Fig. 1b), based on the work of Laitenberger et al. (2014): angulus acromialis, acromioclavicular joint, lateral epicondyle, medial epicondyle, ulnar styloid, radial styloid, 2nd metacarpal distal, 5th metacarpal distal, 2nd metacarpal proximal and 4th metacarpal proximal.

Eight upper limb phantom movements, namely elbow flexion (EF), elbow extension (EE), forearm pronation (FP), forearm supination (FS), wrist flexion (WF), wrist extension (WE), hand open (HO) and hand close (HC), plus a "no movement" (NM) were included in the experiment. Participants sat on a chair, unconstrained, during the recordings. sEMG and kinematic data were recorded in eight consecutive trials. For each trial, one of the 8 phantom movements was randomly chosen. Participants were instructed to produce medium, constant contraction to the best of their ability in the desired direction of motion starting from an initial position. Participants used mirror movements of their intact limb to aid in attempting movements with their residual limb (Jarrasse et al., 2016). The movement was repeated twice and held for 4 s. There was a 3 s resting period between consecutive movements where participants would return to the starting position, which accounted for the NM. All trials were repeated three times, for a total contraction time of 24 s per phantom movement and of 72 s of NM. Ample rest periods were provided between each trial to prevent fatigue. Fig. 2 shows an example of the acquired signals.